inorganics

MDPI

Article

Chiral Amine Covalent Organic Cage Lingated with Copper for Asymmetric Decarboxylative Mannich Reaction

Kaihong Liu [1,2], Chunxia Tan [2] and Lingli Yuan [1,*]

[1] Department of Hematology, The Second Xiangya Hospital, Central South University, 139 Renmin Road, Changsha 410011, China; 1000479980@smail.shnu.edu.cn
[2] Shanghai Frontiers Science Center of Biomimetic Catalysis, Joint Laboratory of International Cooperation of Resource Chemistry of Ministry of Education, Shanghai Normal University, Shanghai 200234, China; tanchx@shnu.edu.cn
* Correspondence: lingliestelle@csu.edu.cn

Abstract

The efficient employment of chiral porous organic cages (POCs) for asymmetric catalysis is of great significance. In this work, we have synthesized a chiral N-rich organic cage constructed through chiral (*S*, *S*)-1,2-cyclohexanediamine and benzene-1,3,5-tricarbaldehyde utilizing dynamic imine chemistry according to the literature. Following reduction with $NaBH_4$, the resulting amine-based POCs (**RCC3**) feature appended chiral diamine moieties capable of coordinating Cu^{2+} cations. This Cu^{2+} coordination provides **RCC3** with excellent enantioselectivity as a supramolecular nanoreactor in asymmetric decarboxylative Mannich reactions, providing up to 94% ee of the product. We found that the spatial distribution of chiral amine sites and the coordination of Cu^{2+} in the **RCC3** have a significant impact on catalytic activity, especially enantioselectivity. This work provides insights into the structure–function relationship within supramolecular catalytic systems

Keywords: covalent organic cage; decarboxylative Mannich reactions; asymmetric catalysis

check for updates

Academic Editor: David Turner

Received: 28 April 2025
Revised: 7 July 2025
Accepted: 14 July 2025
Published: 17 July 2025

Citation: Liu, K.; Tan, C.; Yuan, L. Chiral Amine Covalent Organic Cage Lingated with Copper for Asymmetric Decarboxylative Mannich Reaction. *Inorganics* **2025**, *13*, 245. https://doi.org/10.3390/inorganics13070245

Copyright: © 2025 by the authors. Licensee MDPI, Basel, Switzerland. This article is an open access article distributed under the terms and conditions of the Creative Commons Attribution (CC BY) license (https://creativecommons.org/licenses/by/4.0/).

1. Introduction

In the past decade, imine bond-based covalent organic cages have been among the most popular [1–5]. A typical example was the well-known privileged chiral [4 + 6] cycloimine cage **CC3** [6] reported by Cooper which has been widely employed in fields such as molecular separation [7,8], gas storage [9], and guest encapsulation [10–14]. Given that the imine bond can be reduced into robust amine analogs [15,16], the stability of the corresponding cages can be significantly improved; meanwhile, with an flexible amine bond, inherent tunable porosity, and attractive solubility behavior, the covalent organic cage should be an ideal host for substrate and catalytically active metal salts [17]. In this context, it probably forms a multi-functional catalyst in which the amine bond can induce the preorganization of a substrate while the diamine-ligated metal salt can be used for other metal activation processes.

The asymmetric decarboxylative Mannich reaction (DMR) between β-ketoacids and imines serves as an excellent model for evaluating dual-catalyst systems involving amine cages combined with metal salts. This reaction necessitates the cooperative action of stereochemical regulation and catalytic activation [18–36]. Over the past several decades, the asymmetric catalysis of the DMR has primarily followed two main pathways. The first involves chiral organocatalyst-mediated asymmetric catalysis, where controlling the C=N bond geometry using a chiral organocatalyst is crucial for enantioselectivity. A

representative mechanistic study by the Ma group [37] highlights this approach. Typically, the reaction is conducted at low temperatures (around −20 °C) to enhance enantiomeric excess (ee). The second pathway is a substrate-induced diastereoselective DMR, which proceeds under milder conditions. For instance, the Tian group [38] developed a highly diastereoselective DMR using optically active 2-(tert-butanesulfinyl-imino)glyoxylates as substrates at room temperature. Similarly, the Wang group [39] reported that sulfonamides induced the dimerization of chiral thiourea macrocycles via hydrogen bonding. This dimerization, in turn, activated the sulfonamide and preorganized it in a specific orientation, facilitating nucleophilic attack by β-ketoacids. The cooperative interaction between the two macrocycles significantly enhanced both reactivity and enantioselectivity. Beyond these two main pathways, recent advancements have expanded the scope of asymmetric DMR. The Ma group [40] reported a synergistic catalytic approach using chiral binaphthyl phosphoric acid and copper salts as a dual-catalyst system for the asymmetric DMR of β-ketoacids with α-arylenamides. Meanwhile, the Wang group demonstrated an asymmetric DMR facilitated by an anion–π interaction within a chiral molecular cage [41]. Despite these significant advancements, further exploration of more efficient catalysts based on well-established methodologies remains valuable for enantioselective DMRs. The resulting chiral β-amino ketones are important synthetic intermediates for natural products and biologically active compounds.

Encouraged by the advantages of covalent organic amine cages and the known DMR pathway, we have synthesized an amine covalent organic cage, **RCC3**, by employing aldehyde with (*S*, *S*)-1,2-cyclohexane diamine. The characteristics of this molecular cage reactor lie in the specific functions of chiral cyclohexanediamine: they can coordinate with Cu^{2+} cations to form highly active sites, thereby promoting the formation of intermediates for decarboxylation and the enolization of acetoacetic acid. Meanwhile, adjacent diamine groups provide multiple hydrogen bonds, which can anchor the 1,2,3-Benzoxathiazine-2,2-dioxide substrate at the position adjacent to Cu^{2+}. This spatial advantage will facilitate stereo selective matching with enol intermediates, creating a complex dual site regulatory system that provides the possibility for efficient and enantioselective decarboxylation Mannich reactions.

2. Results and Discussion

The imine cage was first reported by Cooper and coworkers for gas adsorption [2]. It was obtained in a typical synthesis procedure: the aldehydes (L^1) and (*S*, *S*)-1,2-cyclohexane diamine were self-assembled by imine condensation in the solvent at room temperature (Scheme 1). Colorless needle-shaped crystals were isolated from the reaction mixture (73% for **CC3**). Further, the reaction with $NaBH_4$ yielded a reduced **RCC3** nanocage. A sharp peak at 8.19 ppm in the ^{1}H NMR spectrum of **CC3** confirms the formation of imine functionality (Synthesis 2.1 Supplementary Materials). The peak at 4.03 ppm is attributed to the aliphatic -CH_2- units of ethylenediamine, suggesting effective cross-condensation. The peaks at 3.7 ppm and 2.67 ppm in the ^{1}H NMR spectrum of **RCC3** suggest the imine to amine transformation (Synthesis 2.2, Supplementary Materials). The conversion of **CC3** to **RCC3** was further corroborated through FTIR spectroscopy. The disappearance of the C=N peak at about 1636–1647 cm^{-1} and the appearance of new peaks at 3122–3157 and about 1607 cm^{-1} for N-H stretching and C-N-H bending vibration, respectively, indicate the formation of **RCC3** (Figure S1, Supplementary Materials).

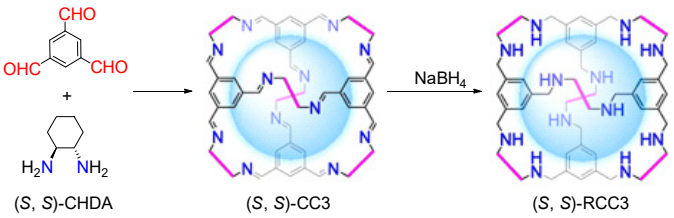

Scheme 1. Synthesis of supramolecular amine cages (*S*,*S*)-**RCC3**.

The targeted amine containers carry diamino donor pockets which potentially provide coordination and hydrogen bonding forces for the encapsulated substrates making them designable and programmable nanoreactors. The coordination capacity of those containers was tested by investigating the binding stoichiometry of the containers (**RCC3**) toward Cu^{2+} through UV-Vis titration (Figure 1). The Job plots of **RCC3** with Cu^{2+} at 288 nm display maximum emission at $[Cu^{2+}]/\{6[\mathbf{RCC3}] + Cu^{2+}\} = 0.4$ (Figure 1), indicating that a 1:4 inclusion copper compound-coordinated **RCC3** porous cage (**RCC3**-Cu) was synthesized by the self-assembly of the reduced **RCC3** with Cu^{2+} in THF.

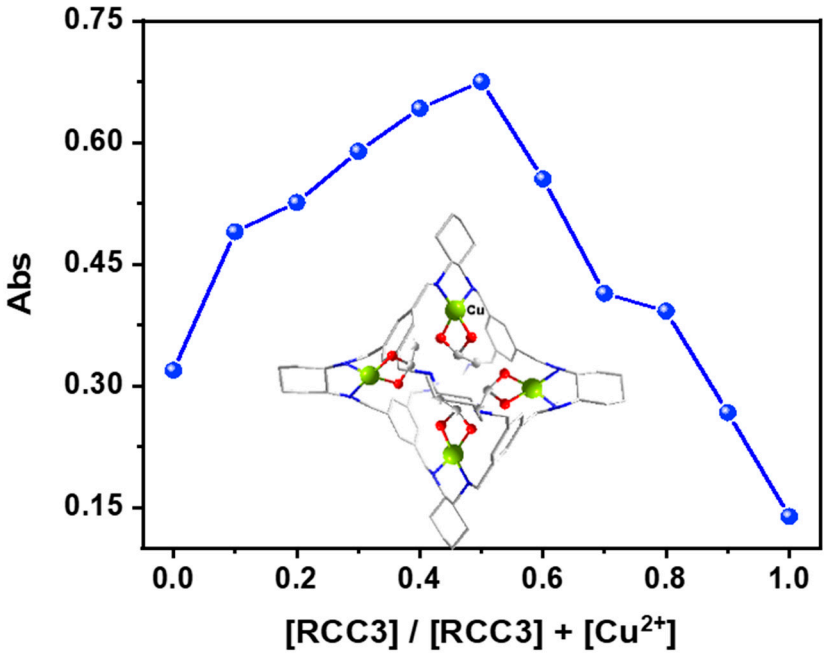

Figure 1. The Job's plot for the determination of the stoichiometry of **RCC3** and $Cu(OAc)_2$ binding.

Asymmetric organocatalysis: The decarboxylative Mannich reaction (DMR), involving a decarboxylative nucleophilic addition to a 1,2,3-Benzoxathiazine-2,2-dioxide, is a general strategy used in the construction of β-sulfonamido ketones, and previous explorations have enabled some enantioselective DMR processes [5]. In particular, the use of a chiral Cu/bisoxazoline complex as a DMR catalyst has exhibited unique advantages [6]; the Ma group utilized it to successfully realize an enantioselective DMR conversion of cyclic ketimines and β-keto acids into the chiral β-sulfonamidoketones [6a]. The unique combination of solution processability and inherent internal voids makes **RCC3** an ideal platform for highly active catalysts. These properties allow efficient access to catalytic centers and promote the transport of reactants and products. The fruitful chiral diamine units endow **RCC3** with the enzyme-mimicking chiral cavity microenvironments which could facilitate the asymmetric aldol reaction.

Our initial investigation began with screening various reaction conditions (Table 1), and the model substrates of 1,2,3-Benzoxathiazine-2,2-dioxide (**1a**) and acetoacetic acid (**2a**). As

shown in Table 1, entry 1–3, when the DMR was catalyzed under 5 mol% of RCC3 with $Cu(OAc)_2$, a 79% yield of the product was obtained with 91% ee under −20 °C. The ee value decreased dramatically when the temperature increased (entry 4). When copper salts of other anions were used together with molecular cages for catalysis, the enantioselectivity still remained at 81–89% (entry 5–8), indicating that anions have little effect on selectivity. However, the proportion of copper salts has a significant impact on the selectivity of the reaction (entry 9–13). As the amount of copper salts increases, the enantioselectivity decreases significantly, possibly due to the coordination between copper salts and amino groups hindering the spatial regulation of hydrogen bonds. Meanwhile, the dynamic monitoring of the reaction showed that the maximum yield was achieved after nearly 6 h of reaction (entry 14–16). After screening various reaction conditions, including catalyst loading, reaction time, temperature, and co-catalyst loading, we found that the best condition for this catalysis system was 5 mol% loading of **RCC3**/$Cu(OAc)_2$ (1/1) which catalyzed the decarboxylative Mannich reaction of 1,2,3-Benzoxathiazine-2,2-dioxide and acetoacetic acid to give a valuable *β*-amino ester at a 79% yield and 91% ee in THF at −20 °C after 6 h.

Table 1. Optimization of DMR process of **1a** and **2a** [a].

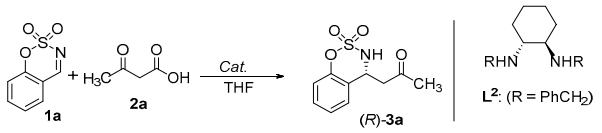

Entry	Cat.	Loading (mol%)	Time	Yield [b]/%	ee [c]/%
1	**RCC3**: $Cu(OAc)_2$ (1:1)	2.5	6	77	86
2	**RCC3**: $Cu(OAc)_2$ (1:1)	5	6	79	91
3	**RCC3**: $Cu(OAc)_2$ (1:1)	10	6	77	90
4	**RCC3**: $Cu(OAc)_2$ (1:1)	5	6	86 [d] (68) [e]	78 [d] (57) [e]
5	**RCC3**: $Cu(OTf)_2$ (1:1)	5	6	79	83
6	**RCC3**: CuBr (1:1)	5	6	78	81
7	**RCC3**: $CuCl_2$ (1:1)	5	6	79	81
8	**RCC3**: CuI_2 (1:1)	5	6	77	89
9	**RCC3**: $Cu(OAc)_2$ (1:2)	5	6	78	55
10	**RCC3**: $Cu(OAc)_2$ (1:3)	5	6	73	60
11	**RCC3**: $Cu(OAc)_2$ (1:4)	5	6	80	55
12	**RCC3**: $Cu(OAc)_2$ (1:5)	5	6	78	55
13	**RCC3**: $Cu(OAc)_2$ (1:6)	5	6	79	57
14	**RCC3**: $Cu(OAc)_2$ (1:1)	5	1	45	91
15	**RCC3**: $Cu(OAc)_2$ (1:1)	5	2	62	88
16	**RCC3**: $Cu(OAc)_2$ (1:1)	5	4.5	76	90

[a] For reaction details see the synthesis section in the Supplementary Materials. [b] Isolated yield. [c] The ee was determined by HPLC analysis. [d] Catalyzed at 0 °C. [e] Catalyzed at *r.t.*

Subsequently, to demonstrate the generality of the chiral container catalysts, we investigated the substrate scope. It was found that 1,2,3-Benzoxathiazine-2,2-dioxide substrates bearing either electron-withdrawing or electron-donating groups (**1a**–**1g**) could react with *β*-ketoacid (**2a**), affording the corresponding products (**3aa**–**3ga**) at good yields (71–79%) and stereoselectivities (50–94% ee). Notably, electron-withdrawing substituents exhibited a lower enantioselectivity: 50% ee for 4-nitro 1,2,3-Benzoxathiazine-2,2-dioxide derivative (**3ga**) (Figure 2a). In the case of *β*-ketoacid substrates, enantioselectivity showed a dependence on both steric size and rigidity. When aliphatic **β**-ketoacids with varying steric hindrance and/or rigidity (**2a**–**2e**) were used, the reaction catalyzed by **RCC3**/$Cu(OAc)_2$

(1:1) provided the products (**3aa**–**3ae**) at a 74–79% yield and 71–87% ee (Figure 2b). Interestingly, enantioselectivity gradually decreased as the steric hindrance and/or rigidity of the alkyl chains increased. This trend was also observed in reactions involving β-ketoacids and ortho-, meta-, and para-substituted cyclic aldimines (Scheme 2), suggesting that the catalytic active site was located within the cavity of **RCC3**. All these results further indicate that the spatial positioning of the keto acid within the confined cavity of **RCC3** plays a crucial role in determining enantioselectivity.

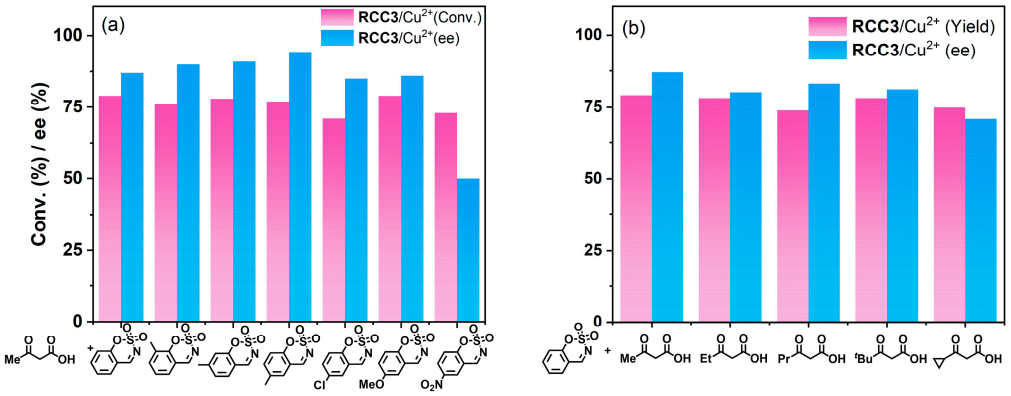

Figure 2. The catalytic results of (**a**) the acetoacetic acid react with substituted 1,2,3-Benzoxathiazine-2,2-dioxide derivatives and (**b**) 1,2,3-Benzoxathiazine-2,2-dioxide react with aliphatic keto acid derivatives.

By comparison, the unreduced cage CC3 showed a significantly worse performance, affording the desired product at just 77% yield and 25% ee. (Table 2, entry 2). These results indicate that the conversion of the imine bond into amine bond plays an important role in the enantioselective control. As the **RCC3** can coordinate with up to four Cu^{2+}, we tested the activity after increasing the amount of $Cu(OAc)_2$ (Table 2, entries 1 & 3–4), which showed that the enantioselectivity decreased as the amount of Cu^{2+} increased, which indicates that the NH- bond plays a key role in enantioselective control. Although the DMR can be catalyzed by pure **CC3** or **RCC3** to yield products, enantioselectivity remains low (5–9% ee, Table 2, entries 5–7) in the absence of a Cu^{2+} co-catalyst, even after a prolonged reaction time (12 h). This low ee demonstrates that the coordinated Cu center also plays a critical role in achieving a high enantioselectivity.

At the same time, the catalytic behavior of the related molecular catalysts of the model compound (1S,2S)-*N*, *N*′-bis(phenylmethyl)-1,2-cyclohexanediamine (PMCHDA, **L0**) were examined (Table 2, entries 7–8). There was nearly no enantioselectivity observed for $\mathbf{L^2}$ and only 47% ee for $Cu(OAc)_2/\mathbf{L^2}$ (1/1). Consistent with reports in the literature [42], the use of R,R-diamine ligands systematically generates the opposite enantiomer compared to S,S-configured analogs in this transformation. These results demonstrate the critical role of the cage structure. The improved enantioselectivity observed with $\mathbf{RCC3}/Cu^{2+}$ is attributed to its chiral cavity NH groups acting cooperatively with $Cu(OAc)_2$. This cooperation facilitates multipoint substrate binding, which directs nucleophilic attack and consequently controls both selectivity and reactivity.

Based on the experimental results, the presence of molecular amine cages and copper salts are key factors regulating the reaction's stereoselectivity. Given that amine cages possess more NH groups than imine cages, providing multiple hydrogen bonding sites, we propose that hydrogen bonding and Cu^{2+} coordination are responsible for the stereoselectivity. Consequently, we propose the plausible reaction mechanism depicted in Figure 3. Initially, substrates **2a** and **1a** enter the molecular cage cavity via host–guest interactions. The acyl group of **2a**, resembling an acetate anion, competes with Cu^{2+} to form complex

RCC3@Cu·**2a**, simultaneously activating **2a** for decarboxylation. Within the confined cavity, the combined action of hydrogen bonding and coordination bonds restricts the approach of **1a** to the activated **2a**, allowing interaction only on the specific face of the C=N with the smallest steric hindrance. This steric constraint results in the formation of the specific stereoselective Mannich product **3aa**.

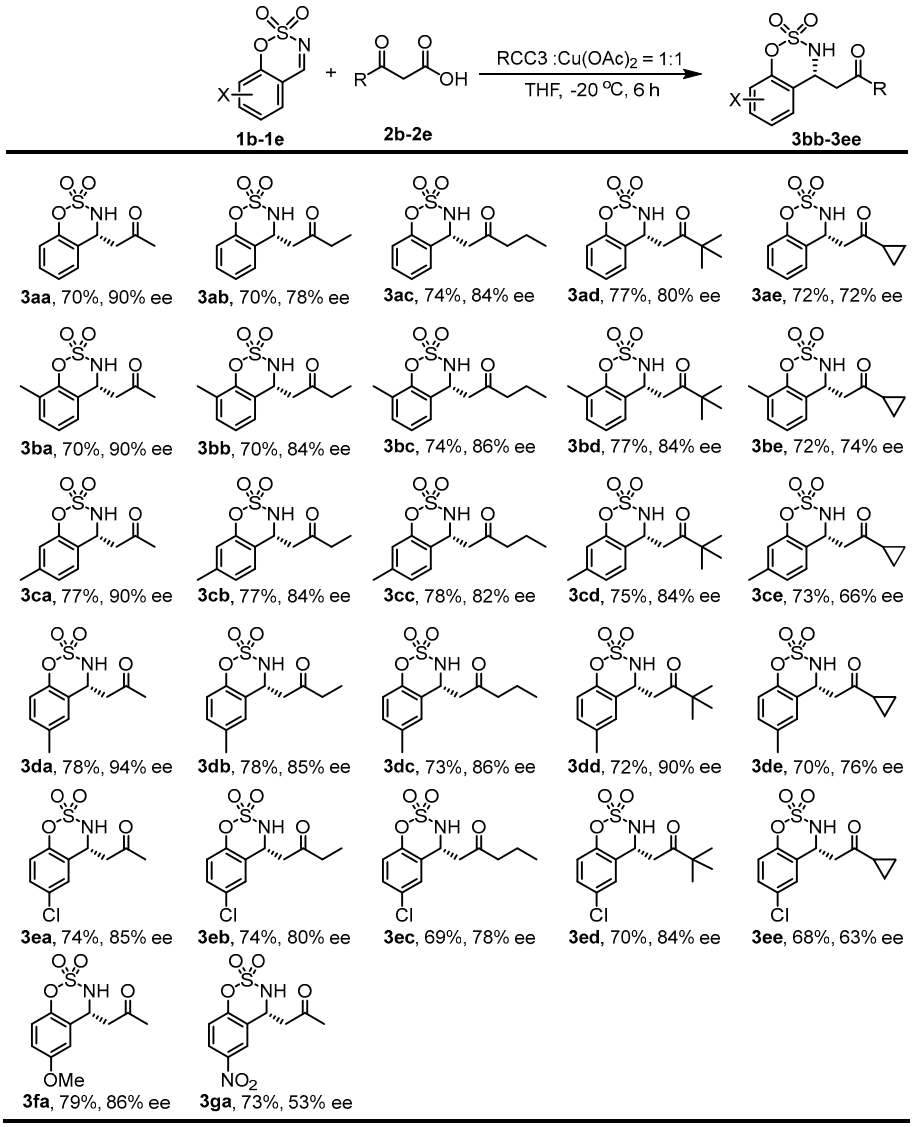

Scheme 2. Substrate scope for the DMR.

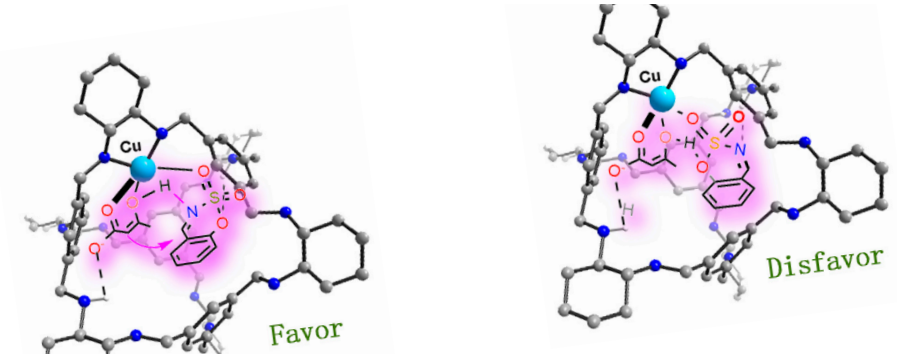

Figure 3. Proposed mechanism for the DMR catalyzed by **RCC3**/$Cu(OAc)_2$ (1:1).

Table 2. Control experiment of DMR Process of **1a** and **2a** [a].

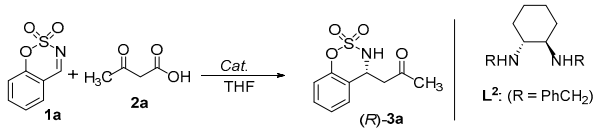

Entry	Cat.	Time	Yield [b]/%	ee [c]/%
1	**RCC3**: $Cu(OAc)_2$ (1:1)	6	79	91
2	**CC3**: $Cu(OAc)_2$ (1:1)	12	77	25
3	**RCC3**: $Cu(OAc)_2$ (1:2)	6	75	90
4	**RCC3**: $Cu(OAc)_2$ (1:4)	6	73	86
5	**CC3**	12	63	5
6	**RCC3**	12	66	9
7	**L²**	12	61	6
8	**L²**: $Cu(OAc)_2$ (1:1)	12	86	47
9	$Cu(OAc)_2$	12	40	0

[a] For reaction details see the synthesis section in the Supplementary Materials. [b] Isolated yield. [c] The ee was determined by HPLC analysis.

3. Materials and Methods

3.1. Materials and General Procedures

All materials and solvents were commercially available and used without further purification. The **RCC3** was synthesized by two steps at a 59.1% overall yield. Fourier transform infrared (FTIR) spectra were collected on a Nicolet Magna 550 spectrometer (Thermo Electron Corporation (now Thermo Fisher Scientific Inc.) in Madison, WI, USA.) using KBr method. UV-vis spectra were recorded with a Hitachi U-3900 Spectrophotometer (Hitachi High-Tech Corporation, Tokyo, Japan) in the wavelength range of 200–800 nm.

3.2. Synthesis of CC3

The synthesis of **CC3** was conducted according to the previous method. A typical procedure is as follows: benzene-1,3,5-tricarbaldehyde (0.5 g) was dissolved in 10.0 mL CH_2Cl_2 in the vessel, and trifluoroacetic acid (10 uL) was added directly to this solution as a catalyst for imine bond formation. Then, 10 mL CH_2Cl_2 solution of (*R*, *R*)-1,2-diamino cyclohexane (0.5 g, 4.464 mmol) was added. The vessel of the mixture solution was capped and left to stand for one week. Crystals grew on the sides of the vessel. The crystalline product was removed by centrifugation and washed with a CH_2Cl_2/CH_3OH mixture (*v*/*v*, 5/95) several times, and further dried at 60 °C under vacuum overnight. The ^1H NMR and ^{13}C NMR spectra were tested to confirm the target structure of **CC3**: ^1H NMR (400 MHz, Chloroform-d) δ 8.19 (s, 1H), 7.94 (s, 1H), 3.36 (d, J = 7.3 Hz, 1H), 1.85 (d, J = 8.6 Hz, 1H), 1.70 (s, 2H), 1.49 (d, J = 10.3 Hz, 1H). ^{13}C NMR (101 MHz, Chloroform-d) δ 159.20, 136.61, 129.63, 74.61, 33.00, 24.37. FT-IR (KBr, cm^{-1}) for **CC3**: 3386(br), 3286(s), 3085(m), 2927(s), 2852(s), 2667(w), 2582(w), 1703(m), 1644(s), 1598(m), 1447(s), 1372(s), 1341(s), 1260(w), 1241(w), 1200(w), 1160(s), 1139(s), 1093(s), 1060(m), 1044(m), 990(m), 936(m), 885(m)854(m), 841(w), 808(w), 688(s), 669(s), 521(m), 477(m).

3.3. Synthesis of Corresponding Reduced RCC3

The imine container (500.0 mg) was dissolved in a CH_2Cl_2/CH_3OH mixture (*v*/*v*, 1/1, 25.0 mL) by stirring. When this solution became clear, $NaBH_4$ (0.5 g) was added and the reaction was stirred for 15 h at room temperature. Water (1.0 mL) was then added,

and the solution was continuously stirred for an additional 9 h. The solvent was then removed under a vacuum. The resulting solid was washed with water and collected by centrifugation, and the obtained solid was dried at 80 C under a vacuum overnight. The ^{1}H NMR and ^{13}C NMR spectra were tested to confirm the target-reduced containers. **RCC3** ^{1}H NMR (400 MHz, Chloroform-d) δ 7.14 (s, 1H), 3.84 (d, J = 14.0 Hz, 1H), 3.58 (d, J = 14.1 Hz, 1H), 2.37 − 2.14 (m, 3H), 2.02 (d, J = 12.5 Hz, 1H), 1.76 − 1.56 (m, 2H), 1.25 − 1.09 (m, 1H), 0.99 (d, J = 11.8 Hz, 1H). ^{13}C NMR (101 MHz, CDCl3) δ 141.22, 125.11, 61.31, 50.63, 31.93, 31.67, 29.71, 24.98. FT-IR (KBr, cm^{-1}) for RCC3: 3297(s), 3153(br), 3004(w), 2928(s), 2847(s), 2666(w), 1686(w), 1646(s), 1451(s), 1399(m), 1359(w), 1333(w), 1263(w), 1239(w), 1206(w), 1157(m), 1115(s), 1056(w), 1030(w), 999(m), 948(w), 854(m), 795(m), 713(w), 525(w).

3.4. General Procedure for DMR

In a typical procedure, 5 mol% of **RCC3** (22 mg, 0.02 mmol) and $Cu(OAc)_2$ (3.6 mg, 0.02 mmol) were well dispersed into 4.0 mL of THF and stirred for 6 h. Subsequently, the benzo[e][1,2,3]oxathiazine 2,2-dioxide (18.3 mg, 0.1 mmol) and acetoacetic acid (24.6 mg, 0.15 mmol) were added into the mixture at −20 °C. The mixture was stirred for another 6 h and then filtered through a silica plug and washed with Et_2O (5.0 mL). The filtrate was analyzed by chiral HPLC and ^{1}H NMR for enantioselectivity and conversion, respectively.

4. Conclusions

In summary, we have successfully applied the amino chiral covalent organic cage **RCC3** catalytic system to the asymmetric decarboxylation Mannich reaction between β—ketoacids and cyclic aldimines. Compared with the corresponding monomeric catalysts, the co-catalysis of **RCC3** with $Cu(OAc)_2$ exhibits enhanced stereoselectivity and comparable activity in DMR. The control experiments of amine/imine cages or imine cages coordinating with $Cu(OAc)_2$ indicate that the hydrogen bonding of amine cages and the presence of Cu^{2+} have important effects on the regulation of stereoselectivity. This study indicates that POCs can provide a multifunctional composite catalytic platform for organic reactions as catalysts.

Supplementary Materials: The following supporting information can be downloaded at: https://www.mdpi.com/article/10.3390/inorganics13070245/s1, Figure S1: IR spectra; Figure S2: Job Plots; Table S1: Additional catalystic results; Figure S3: HPLC; Figure S4: NMR spectra for substrate scope.

Author Contributions: C.T. initiated the concept. K.L. performed the experiments and collected the data. L.Y. and C.T. analyzed the data. C.T. provided the main funding for this work. L.Y. wrote and edited the paper. All authors have read and agreed to the published version of the manuscript.

Funding: This research was funded by the China National Natural Science Foundation (22001171,81600140), Hunan National Natural Science Foundation (2023JJ30800), the Shanghai Rising-Star Program (23QA1407200), the Sailing Program (2020YF1435200), the Shanghai STDF (20070502600), and the Shanghai Frontiers Science Center of Biomimetic Catalysis for financial support.

Data Availability Statement: The data supporting this article have been included as part of the Supplementary Materials.

Conflicts of Interest: The authors declare no conflicts of interest.

References

1. Yang, X.; Ullah, Z.; Stoddart, J.F.; Yavuz, C.T. Porous Organic Cages. *Chem. Rev.* **2023**, *123*, 4602–4634. [CrossRef]
2. Hasell, T.; Little, M.A.; Chong, S.Y.; Schmidtmann, M.; Briggs, M.E.; Santolini, V.; Jelfs, K.E.; Cooper, A.I. Chirality as a tool for function in porous organic cages. *Nanoscale* **2017**, *9*, 6783–6790. [CrossRef]
3. Gao, W.B.; Li, Z.H.; Tong, T.Y.; Dong, X.; Qu, H.; Yang, L.L.; Sue, A.C.H.; Tian, Z.Q.; Cao, X.Y. Chiral Molecular Cage with Tunable Stereoinversion Barriers. *J. Am. Chem. Soc.* **2023**, *145*, 17795–17804. [CrossRef]

4. Zhou, H.; Ao, Y.F.; Wang, D.X.; Wang, Q.Q. Inherently Chiral Cages via Hierarchical Desymmetrization. *J. Am. Chem. Soc.* **2022**, *144*, 16767–16772. [CrossRef]
5. Liu, C.; Jin, Y.; Qi, D.; Ding, X.; Ren, H.; Wang, H.; Jiang, J. Enantioselective assembly and recognition of heterochiral porous organic cages deduced from binary chiral components. *Chem. Sci.* **2022**, *13*, 7014–7020. [CrossRef]
6. Monta-González, G.; Sancenón, F.; Martínez-Mán, R.; MartíCentelles, V. Purely Covalent Molecular Cages and Containers for Guest Encapsulation. *Chem. Rev.* **2022**, *122*, 13636–13708. [CrossRef]
7. Tozawa, T.; Jones, J.T.A.; Swamy, S.I.; Jiang, S.; Adams, D.J.; Shakespeare, S.; Clowes, R.; Bradshaw, D.; Hasell, T.; Chong, S.Y.; et al. Porous organic cages. *Nat. Mater.* **2009**, *8*, 973–978. [CrossRef] [PubMed]
8. Bhandari, P.; Mukherjee, P.S. Covalent Organic Cages in Catalysis. *ACS Catal.* **2023**, *13*, 6126–6143. [CrossRef]
9. Du, Y.-J.; Zhou, J.-H.; Tan, L.-X.; Liu, S.-H.; Zhao, K.; Gao, Z.-M.; Sun, J.-K. Porous Organic Cage Nanostructures for Construction of Complex Sequential Reaction Networks. *ACS Appl. Nano Mater.* **2022**, *5*, 7974–7982. [CrossRef]
10. Yang, X.-D.; Tan, L.; Sun, J.-K. Encapsulation of Metal Clusters within Porous Organic Materials: From Synthesis to Catalysis Applications. *Chem. Asian J.* **2022**, *17*, e202101289. [CrossRef]
11. Wang, Y.; Sun, Y.B.; Shi, P.C.; Sartin, M.M.; Lin, X.J.; Zhang, P.; Fang, H.X.; Peng, P.X.; Tian, Z.Q.; Cao, X.Y. Chaperone-like chiral cages for catalyzing enantio-selective supramolecular polymerization. *Chem. Sci.* **2019**, *10*, 8076–8082. [CrossRef] [PubMed]
12. Xu, N.; Su, K.Z.; El-Sayed, E.S.M.; Ju, Z.F.; Yuan, D.Q. Chiral proline-substituted porous organic cages in asymmetric organocatalysis. *Chem. Sci.* **2022**, *13*, 3582–3588. [CrossRef] [PubMed]
13. Zhang, D.W.; Dutasta, J.P.; Dufaud, V.; Guy, L.; Martinez, A. Sulfoxidation inside a C_3-Vanadium(V) Bowl-Shaped Catalyst. *ACS Catal.* **2017**, *7*, 7340–7345. [CrossRef]
14. Wang, K.; Tang, X.; Anjali, B.A.; Dong, J.; Jiang, J.; Liu, Y.; Cui, Y. Chiral Covalent Organic Cages: Structural Isomerism and Enantioselective Catalysis. *J. Am. Chem. Soc.* **2024**, *146*, 6638–6651. [CrossRef] [PubMed]
15. Gao, S.Q.; Liu, Y.T.; Wang, L.H.; Wang, Z.H.; Liu, P.B.; Gao, J.; Jiang, Y.J. Incorporation of Metals and Enzymes with Porous Imine Molecule Cages for Highly Efficient Semiheterogeneous Chemoenzymatic Catalysis. *ACS Catal.* **2021**, *11*, 5544–5553. [CrossRef]
16. Zhang, S.-Y.; Kochovski, Z.; Lee, H.-C.; Lu, Y.; Zhang, H.; Zhang, J.; Sun, J.-K.; Yuan, J. Ionic organic cage-encapsulating phase-transferable metal clusters. *Chem. Sci.* **2019**, *10*, 1450–1456. [CrossRef]
17. Lu, Y.-L.; Qin, Y.-H.; Zheng, S.-P.; Ruan, J.; Huang, Y.-H.; Zhang, X.-D.; Liu, C.-H.; Hu, P.; Xu, H.-S.; Su, C.-Y. Anion-Mediated Allosteric Catalysis of [2 + 2] Photocycloaddition Based on a Flexible Metallo-Amine Cage for High Diastereoselectivity. *ACS Catal.* **2024**, *14*, 94–103. [CrossRef]
18. Saha, R.; Mondal, B.; Mukherjee, P.S. Molecular Cavity for Catalysis and Formation of Metal Nanoparticles for Use in Catalysis. *Chem. Rev.* **2022**, *122*, 12244–12307.
19. Wang, Z.-L. Recent Advances in Catalytic Asymmetric Decarboxylative Addition Reactions. *Adv. Synth. Catal.* **2013**, *355*, 2745–2755. [CrossRef]
20. Nakamura, S. Catalytic enantioselective decarboxylative reactions using organocatalysts. *Org. Biomol. Chem.* **2014**, *12*, 394–405. [CrossRef]
21. Evans, D.A.; Mito, S.; Seidel, D. Scope and Mechanism of Enantioselective Michael Additions of 1,3-Dicarbonyl Compounds to Nitroalkenes Catalyzed by Nickel(II)–Diamine Complexes. *J. Am. Chem. Soc.* **2007**, *129*, 11583–11592. [CrossRef] [PubMed]
22. Zheng, Y.; Xiong, H.-Y.; Nie, J.; Hua, M.-Q.; Ma, J.-A. Biomimetic catalytic enantioselective decarboxylative aldol reaction of β-ketoacids with trifluoromethyl ketones. *Chem. Commun.* **2012**, *48*, 4308–4310. [CrossRef] [PubMed]
23. Yang, C.-F.; Shen, C.; Wang, J.-R.; Tian, S.-K. A Highly Diastereoselective Decarboxylative Mannich Reaction of β-Keto Acids with Optically Active *N*-Sulfinyl α-Imino Esters. *Org. Lett.* **2012**, *14*, 3092–3095. [CrossRef]
24. Zhong, F.; Yao, W.; Dou, X.; Lu, Y. Enantioselective Construction of 3-Hydroxy Oxindoles via Decarboxylative Addition of β-Ketoacids to Isatins. *Org. Lett.* **2012**, *14*, 4018–4021. [CrossRef]
25. Zuo, J.; Liao, Y.-H.; Zhang, X.-M.; Yuan, W.-C. Organocatalyzed Enantioselective Decarboxylative Stereoablation Reaction for the Construction of 3,3′-Disubstituted Oxindoles Using β-Ketoacids and 3-Halooxindoles. *J. Org. Chem.* **2012**, *77*, 11325–11332. [CrossRef]
26. Moon, H.W.; Kim, D.Y. Enantioselective decarboxylative Michael addition of β-ketoacids to nitroalkenes catalyzed by binaphthyl-derived organocatalysts. *Tetrahedron Lett.* **2012**, *53*, 6569–6572. [CrossRef]
27. Yuan, H.-N.; Wang, S.; Nie, J.; Meng, W.; Yao, Q.; Ma, J.-A. Hydrogen-Bond-Directed Enantioselective Decarboxylative Mannich Reaction of β-Ketoacids with Ketimines: Application to the Synthesis of Anti-HIV Drug DPC 083. *Angew. Chem. Int. Ed.* **2013**, *52*, 3869–3873. [CrossRef]
28. Kang, Y.K.; Lee, H.J.; Moon, H.W.; Kim, D.Y. Organocatalytic enantioselective decarboxylative Michael addition of b-ketoacids to a,b-unsaturated ketones. *RSC Adv.* **2013**, *3*, 1332–1335. [CrossRef]
29. Suh, C.W.; Chang, C.W.; Choi, K.W.; Lim, Y.J.; Kim, D.Y. Enantioselective decarboxylative aldol addition of β-ketoacids to isatins catalyzed by binaphthyl-modified organocatalyst. *Tetrahedron Lett.* **2013**, *54*, 3651–3654. [CrossRef]

30. Zhu, B.-H.; Zheng, J.-C.; Yu, C.-B.; Sun, X.-L.; Zhou, Y.-G.; Shen, Q.; Tang, Y. One-Pot Highly Diastereoselective Synthesis of *cis*-Vinylaziridines via the Sulfur Ylide-Mediated Aziridination and Palladium(0)-Catalyzed Isomerization. *Org. Lett.* **2010**, *12*, 504–507. [CrossRef]
31. Luo, Y.; Carnell, A.J.; Lam, H.W. Enantioselective Rhodium-Catalyzed Addition of Potassium Alkenyltrifluoroborates to Cyclic Imines. *Angew. Chem. Int. Ed.* **2012**, *51*, 6762–6766. [CrossRef]
32. Luo, Y.; Hepburn, H.B.; Chotsaeng, N.; Lam, H.W. Enantioselective Rhodium-Catalyzed Nucleophilic Allylation of Cyclic Imines with Allylboron Reagents. *Angew. Chem. Int. Ed.* **2012**, *51*, 8309–8313. [CrossRef]
33. Zhang, H.; Jiang, C.; Tan, J.-P.; Hu, H.-L.; Chen, Y.; Ren, X.; Zhang, H.-S.; Wang, T. Highly Enantioselective Construction of Fully Substituted Stereocenters Enabled by In Situ Phosphonium-Containing Organocatalysis. *ACS Catal.* **2020**, *10*, 5698–5706. [CrossRef]
34. Zhang, H.-X.; Nie, J.; Cai, H.; Ma, J.-A. Cyclic Aldimines as Superior Electrophiles for Cu-Catalyzed Decarboxylative Mannich Reaction of β-Ketoacids with a Broad Scope and High Enantioselectivity. *Org. Lett.* **2014**, *16*, 2542–2545. [CrossRef] [PubMed]
35. Qian, P.; Dai, Y.; Mei, H.; Soloshonok, V.A.; Han, J.; Pan, Y. Ni-catalyzed asymmetric decarboxylative Mannich reaction for the synthesis of β-trifluoromethyl-β-amino ketones. *RSC Adv.* **2015**, *5*, 26811–26814. [CrossRef]
36. Zhang, H.-J.; Xie, Y.-C.; Yin, L. Copper(I)-catalyzed asymmetric decarboxylative Mannich reaction enabled by acidic activation of 2*H*-azirines. *Nat. Commun.* **2019**, *10*, 1699. [CrossRef]
37. Liu, Y.-J.; Li, J.-S.; Nie, J.; Ma, J.-A. Organocatalytic Asymmetric Decarboxylative Mannich Reaction of β-Keto Acids with Cyclic α-Ketiminophosphonates: Access to Quaternary α-Aminophosphonates. *Org. Lett.* **2018**, *20*, 3643–3646. [CrossRef]
38. Xavier, T.; Condon, S.; Pichon, C.; Le Gall, E.; Presset, M. Decarboxylative Mannich Reactions with Substituted Malonic Acid Half-Oxyesters. *J. Org. Chem.* **2021**, *86*, 5452–5462. [CrossRef]
39. Guo, H.; Zhang, L.-W.; Zhou, H.; Meng, W.; Ao, Y.-F.; Wang, D.-X.; Wang, Q.-Q. Substrate-Induced Dimerization Assembly of Chiral Macrocycle Catalysts toward Cooperative Asymmetric Catalysis. *Angew. Chem. Int. Ed.* **2020**, *59*, 2623–2627. [CrossRef]
40. Tang, X.; Hou, Y.D.; Tan, X.F.; Nie, J.; Cheung, C.W.; Ma, J.A. Synergistic Catalytic Asymmetric Decarboxylative Mannich Reaction of β-Ketoacids with Acyclic α-Arylenamides. *ACS Catal.* **2024**, *14*, 9701–9707. [CrossRef]
41. Luo, N.; Ao, Y.F.; Wang, D.X.; Wang, Q.Q. Exploiting Anion–π Interactions for Efficient and Selective Catalysis with Chiral Molecular Cages. *Angew. Chem. Int. Ed.* **2021**, *60*, 20650–20655. [CrossRef]
42. Zhu, Y.; Wang, H.; Liu, R.; Liu, K.; Hu, X.; Huang, J.; Wang, C.; Wang, L.; Liu, Y.; Liu, G.; et al. Copper(II)-catalyzed enantioselective decarboxylative Mannich reaction coordinated by supramolecular organic amine cages. *Chem. Sci.* **2025**, *16*, 4374–4382. [CrossRef]

Disclaimer/Publisher's Note: The statements, opinions and data contained in all publications are solely those of the individual author(s) and contributor(s) and not of MDPI and/or the editor(s). MDPI and/or the editor(s) disclaim responsibility for any injury to people or property resulting from any ideas, methods, instructions or products referred to in the content.